The American Journal of Pathology, Vol. 181, No. 3, September 2012

http://dx.doi.org/10.1016/j.ajpath.2012.05.032

Immunopathology and Infectious Diseases

TGF-β–Responsive Myeloid Cells Suppress Type 2 Immunity and Emphysematous Pathology after Hookworm Infection

Lisa Heitmann,* Reena Rani,† Lucas Dawson,† Charles Perkins,† Yanfen Yang,† Jordan Downey,† Christoph Hölscher,* and De'Broski R. Herbert†

From Infection Immunology, Research Center Borstel, Borstel, Germany; and the Division of Immunobiology,† Cincinnati Children's Research Foundation, Cincinnati, Ohio*

Transforming growth factor β (TGF-β) regulates inflammation, immunosuppression, and wound-healing cascades, but it remains unclear whether any of these functions involve regulation of myeloid cell function. The present study demonstrates that selective deletion of TGF-βRII expression in myeloid phagocytes i) impairs macrophage-mediated suppressor activity, ii) increases baseline mRNA expression of proinflammatory chemokines/cytokines in the lung, and iii) enhances type 2 immunity against the hookworm parasite *Nippostrongylus brasiliensis*. Strikingly, TGF-β–responsive myeloid cells promote repair of hookworm-damaged lung tissue, because *LysM^{Cre}TGF-βRII$^{flox/flox}$* mice develop emphysema more rapidly than wild-type littermate controls. Emphysematous pathology in *LysM^{Cre}TGF-βRII$^{flox/flox}$* mice is characterized by excessive matrix metalloprotease (MMP) activity, reduced lung elasticity, increased total lung capacity, and dysregulated respiration. Thus, TGF-β effects on myeloid cells suppress helminth immunity as a consequence of restoring lung function after infection. *(Am J Pathol 2012, 181:897–906; http://dx.doi.org/10.1016/j.ajpath.2012.05.032)*

Transforming growth factor β (TGF-β) constitutes a superfamily of molecules that regulate cellular proliferation, differentiation, and survival of hematopoietic and nonhematopoietic lineages.[1,2] TGF-β1, TGF-β2, and TGF-β3 mediate their biological effects through transforming growth factor-beta receptor type II (TGF-βRII), which facilitates Smad-dependent and Smad-independent gene transcription.[3] The immunosuppressive role for TGF-β is well established, in that mice lacking expression of TGF-βRII in all hematopoietic cells or specifically in T cells develop lethal multiorgan inflammatory disease.[4–7] This cytokine also regulates tissue remodeling and fibrosis through mechanisms that involve stromal cells and fibroblasts.[8] Whether TGF-β–dependent effects on myeloid lineage cells serve important roles in immunosuppression and mucosal repair remains entirely unclear.[9–11]

Given that TGF-β suppresses T-lymphocyte effector functions, this cytokine may promote the chronicity of helminth infestations through suppressing T_H2-dominated immune responses.[7,12–14] Indeed, some parasitic helminths produce TGF-β–like molecules in their excretions, exemplifying the importance of this cytokine in host-pathogen interactions.[15] In addition, TGF-β promotes extracellular matrix deposition that may serve as a mechanism to limit excess organ damage in worm-infected hosts.[16,17] For example, the murine hookworm parasite *Nippostrongylus brasiliensis* causes severe hemorrhagic lung injury within days of infection.[18] Worm egress between 3 and 5 days after infection is followed by progressive airway remodeling and fibrosis that resembles certain pathophysiological features of murine asthma.[19] Moreover, *N. brasiliensis*-infected mice develop an emphysematous-like pathology beyond 150 days after infection, characterized by matrix metalloprotease (MMP) production from alternatively activated macrophages (AAMϕ).[20] Whether TGF-β serves any role in host immunity and/or tissue immunopathology after *N. brasiliensis* infection has not been tested.

For the present study, mice deficient for TGF-βRII expression in macrophages and neutrophils were generated (*LysM^{Cre}TGF-βRII$^{flox/flox}$*) to test whether TGF-β–dependent effects on myeloid lineage cells regulated type 2 immunity and pulmonary repair after *N. brasiliensis* infection. Data presented here indicate that *LysM^{Cre}TGF-*

Supported in part by NIH grants R01-AI095289 and R01-GM083204 (D.R.H.).

Accepted for publication May 30, 2012.

Current address of D.R.H., Division of Experimental Medicine, University of California San Francisco, San Francisco, CA.

Address reprint requests to De'Broski R. Herbert, Ph.D., Cincinnati Children's Research Foundation, 3333 Burnet Ave., Cincinnati, OH 45229. E-mail: debroski.herbert@cchmc.org.

βRII$^{flox/flox}$ mice failed to suppress antigen-specific T cell proliferation and T_H2-dominated inflammation, which was associated with reduced worm egg production. The infection-induced expression of AAMϕ-associated genes (*Retnla*, encoding RELMα, and *Arg1*, encoding arginase I) and extracellular matrix deposition (collagen and fibronectin) were moderately affected in the absence of TGF-β–responsive myeloid cells. However, *LysM*^{Cre}*TGF-βRII*$^{flox/flox}$ mice had marked defects in pulmonary tissue repair characterized by dysregulated matrix metalloprotease activity and emphysematous pathology, which demonstrates a previously unrecognized mechanism for TGF-β effects on myeloid cells in regulating immunity and wound healing after hookworm infection.

Materials and Methods

Mice and Parasites

All experiments used sex- and age-matched mice on a wild-type (WT) C57/BL6 background. *TGF-βRII*$^{flox/flox}$ mice (strain number 01XN5) were obtained from the National Cancer Institute mouse repository.[21] *LysM*^{Cre} mice on a WT C57/BL6 background were obtained from the Jackson Laboratory (Bar Harbor, ME). These strains were intercrossed to generate *LysM*^{Cre}*TGF-βRII*$^{flox/flox}$ and *TGF-βRII*$^{flox/flox}$ strains. *N. brasiliensis* was maintained in the laboratory using established protocols. Naïve mice were inoculated subcutaneously with 750 infectious third-stage larvae (L_3). Worm burdens were assessed by opening mouse intestines longitudinally and incubating them in PBS at 37°C for 3 hours in a modified Baermann apparatus, in which tissues were placed in a sieve atop a 250-mL beaker. Parasites that collected at the bottom were counted. For fecal egg counts, feces were collected, weighed, and incubated in saturated NaCl solution; eggs counted using McMaster slides, as described previously.[22] The Institutional Animal Care and Use Committee at the Cincinnati Children's Hospital Medical Center approved all procedures.

Lung Histopathology

To assess airway inflammation, lungs were excised and fixed in 10% formalin, washed in methanol, dehydrated, and embedded in paraffin and cut into 5-μm sections. Sections were mounted on slides and stained with H&E or Masson's trichrome as prepared at the Cincinnati Children's Hospital Medical Center morphology core facility. The left lung was removed and fixed in 10% neutral buffered formalin. Lungs were bisected and oriented cut side down in a paraffin block such that sections would reveal cross-sections of consistent airways for comparison. A Nikon Eclipse E600 microscope fitted with a 40× objective lens (Nikon Plan Apo) was used for image acquisition; photos were captured with a SPOT Diagnostics RT slider digital color camera using a SPOT Diagnostics imaging system (Sterling Heights, MI). Hydroxyproline measurements were performed as described previously.[23]

ELISA and Real-Time PCR

RNA was treated with DNase I, and cDNA was prepared using SuperScript II Reverse Transcriptase (Life Technologies-Invitrogen, Carlsbad, CA). Real-time PCR was performed on a GeneAmp 7500 instrument (Life Technologies-Applied Biosystems, Foster City CA) with SYBR Green detection reagent. For the genes evaluated, C_T values were determined and expressed using the $1/\Delta\Delta CT$ method, as described previously.[12] The mouse wound-healing RT^2 Profiler quantitative RT-PCR array was used to evaluate the expression of genes relevant to the wound-healing response, according to the manufacturer's instructions (SABiosciences, Frederick, MD). Pooled cDNA samples from three individual mice were used for analysis.

Mouse cytokine enzyme-linked immunosorbent assay (ELISA) kits specific for IL-13 and TGF-β were obtained from eBioscience (San Diego, CA). Total MMP activity was determined by a commercially available fluorometric assay (Enzo Life Sciences, Farmingdale, NY).

Flow Cytometric Analyses

Single-cell suspensions of lung tissue or bone marrow-derived macrophage (BMDM)-T cell cocultures were stained with one or more of the following fluorescently labeled monoclonal antibodies (mAbs): anti-mouse TGF-βRII (R&D Systems), anti-mouse CD25 (clone 7D4), anti-mouse CD68 (FA-11), anti-mouse CD11c (clone N418), CD11b (clone M1/70), CD45 (clone 30-F11), and isotype control (MOPC-173) (eBioscience). Intracellular bromodeoxyuridine (BrdU) staining was performed according to the manufacturer's instructions (BD Biosciences, San Jose, CA). Acquisition was performed with a FACSCalibur cell sorting system (BD Biosciences, San Jose, CA), and data were analyzed with FlowJo software (v8.8; Tree Star, Ashland, OR).

Isolation of Lung Tissue Cells and Bronchoalveolar Lavage Fluid Collection

Lungs were perfused with 1× PBS and minced with scissors, followed by digestion in serum-free RPMI 1640 medium containing Liberase CI (0.5 mg/mL; Roche, Indianapolis, IN) and DNase I (0.5 mg/mL; Sigma-Aldrich, St. Louis, MO) RPMI 1640 medium for 30 minutes at 37°C with shaking. Samples were further disassociated by repeated passage through a 10-mL syringe fitted with an 18-gauge needle and finally passed through a 70-mm cell strainer to obtain a single-cell suspension. For cytokine measurements, bronchoalveolar lavage fluid (BALF) was collected using established protocols followed by concentration with Amicon Ultra centrifugal filter units with molecular weight cutoff at 3000 daltons (Millipore, Billerica, MA).

In Vivo *Cytokine Capture Assays*

Relative amounts of *in vivo* IL-4, IFN-γ, and IL-10 secretion were determined by an *in vivo* cytokine capture assay.[24] Injected biotin-labeled anti-cytokine mAbs in this assay form complexes with the secreted cytokines they specifi-

cally bind that have a much longer *in vivo* half-life than free cytokines. Consequently, the complexes accumulate *in vivo* and can be measured by ELISA, using wells coated with mAbs that bind to an epitope on the cytokine that is not blocked by the injected mAb. Bound biotin-mAb/cytokine complexes are detected with horseradish peroxidase-streptavidin, followed by a luminogenic substrate.

OTII-BMDM Coculture

$CD4^+$ cells were isolated from naïve ovalbumin-specific T cell receptor transgenic mice (OTII), as described previously.[12] BMDMs were generated from 6-day culture supernatant from a macrophage colony-stimulating factor (M-CSF)-secreting cell line. BMDMs were either left untreated or exposed to recombinant human TGF-β (endotoxin values of <0.1 ng/mL; PeproTech, Rocky Hill, NJ) for 16 hours, then pulsed with 50 μg/well endotoxin-free chicken egg ovalbumin for 8 hours, washed several times, and cocultured with purified naïve OT-II $CD4^+$ cells at a ratio of 10:1 ($CD4^+$/Mϕ) for 72 to 96 hours. At 16 hours before harvest, 10 mg/mL BrdU was added to cultures.

Measurement of Airway Physiology

Unrestrained whole-body plethysmograph chambers (Buxco Research Systems, Wilmington, NC) were used to evaluate pulmonary airflow in the upper and lower respiratory tract. In this approach, chamber pressure measures the difference between expansion of the thoracic cavity and the volume of air removed from (or added to) the chamber during inspiration (or expiration). Exposure of mice to increasing doses of methacholine was used to determine the enhanced pause response. Invasive measurements of airway responsiveness were made on a flexiVent apparatus (Scientific Respiratory Equipment, Montreal, QC, Canada). Mice were anesthetized with xylazine and sodium pentobarbital. The mice were placed on a rectal thermometer-controlled heating pad to maintain body temperature at 37°C. Mouse tracheas were cannulated with an 18-gauge blunt needle, and the mice were ventilated at 150 breaths/minute and 3.0 cm water positive end expiratory pressure. Mice were paralyzed with 0.8 mg/kg pancuronium bromide and allowed to stabilize on the ventilator for 2 minutes.

Two total lung capacity perturbations were then performed for airway recruitment before baseline measurement. Measurements were made using a 1.25-second, 2.5-Hz volume-driven oscillation applied to the airways by a computer-controlled piston (snapshot perturbation). Newtonian resistance (R_N), inertance (I), tissue damping (G), and tissue elastance (H) were determined by fitting the data to a constant phase model of airway mechanics. Tissue elasticity was calculated from the constant-phase model, which applies fixed-amplitude, wide-frequency (0.25 to 20 Hz) waves to lungs and allows this model to differentiate between the mechanical properties of the airways and the lung tissue. Total lung capacity was calculated from one parameter of the Salazar-Knowles equation[25] (fitting data from PV-loops) that represents the total lung capacity on the total volume axis.

Statistical Analysis

Statistical significance was assessed by either two-tailed Student's *t*-test (two groups) or analysis of variance (analysis of variance) for multiple groups with a post hoc Tukey's test to determine significance. $P \leq 0.05$ was considered significant. All analyses were performed using Prism GraphPad 4.0 software (GraphPad Software, La Jolla, CA).

Results

Mϕ-TGF-βRIIKO Mice Delete TGF-βRII on Alveolar Macrophages and Have a Baseline Increase of Lung Inflammation

Tissue-specific deletion of TGF-β signaling components in mice has greatly increased our understanding of hematopoietic and nonhematopoietic cell regulation.[7,26,27] To investigate the role of TGF-β in myeloid lineage cells, C57BL/6 mice expressing a LoxP-flanked TGF-βRII allele[21] were intercrossed with a mouse strain that expresses Cre recombinase under control of the lysozyme M promoter.[24] Progeny with a $LysM^{Cre}GF\text{-}\beta RII^{flox/flox}$ (hereafter referred to as Mϕ-TGF-βRIIKO mice) genotype were compared with their littermate $LysM^{Cre}$-negative $TGF\text{-}\beta RII^{flox/flox}$ mice (hereafter referred to as WT mice) throughout our studies.

TGF-βRII deletion efficiency in myeloid cells was evaluated in cell suspensions of lung tissue from naïve WT and Mϕ-TGF-βRIIKO mice. Anti-mouse mAbs specific for CD45, CD68, CD11c, and TGF-βRII were used for evaluation via flow cytometry. $FSC^{high}SSC^{low}$ gated cells that coexpressed CD45 and CD68, revealed two distinct populations that were either $CD11c^{high}$ or $CD11c^{low}$ (Figure 1A). Although the $CD11c^{high}$ population in Mϕ-TGF-βRIIKO mice expressed a threefold lower level of TGF-βRII than WT mice, there were no differences in TGF-βRII levels between strains in the $CD11c^{low}$ population (Figure 1, A and B). This indicated that alveolar macrophages had TGF-βRII expression, as these cells express high levels of CD11c, compared with intermediate CD11c levels on lung dendritic cells.[28,29]

Lung tissues of naïve Mϕ-TGF-βRIIKO mice had a relative greater number of $FSC^{low}SSC^{high}$ cells than WT mice (Figure 1A), indicative of a baseline increase in granulocytic inflammation. To further evaluate naïve Mϕ-TGF-βRIIKO mice, a commercially available quantitative RT-PCR-based cDNA array was used to assess inflammatory and tissue repair genes (Figure 1C). Results showed that Mϕ-TGF-βRIIKO mice generated a more than twofold increased expression of chemokine genes (*Ccl12*, *Ccl7*, *Cxcl1*, *Cxcl3*, and *Cxcl5*), granulocyte colony stimulating factor (*Csf3*), and cytokine genes (*Il10* and *Ifng*), compared with WT mice (Figure 1C). In contrast, Mϕ-TGF-βRIIKO mice showed a marked down-regulation of epidermal growth factor (*Egf*), an epithelial cell growth and mucosal repair gene (Figure 1C). Altogether, alveolar macrophages and not dendritic cells in the lungs of Mϕ-TGF-βRIIKO mice

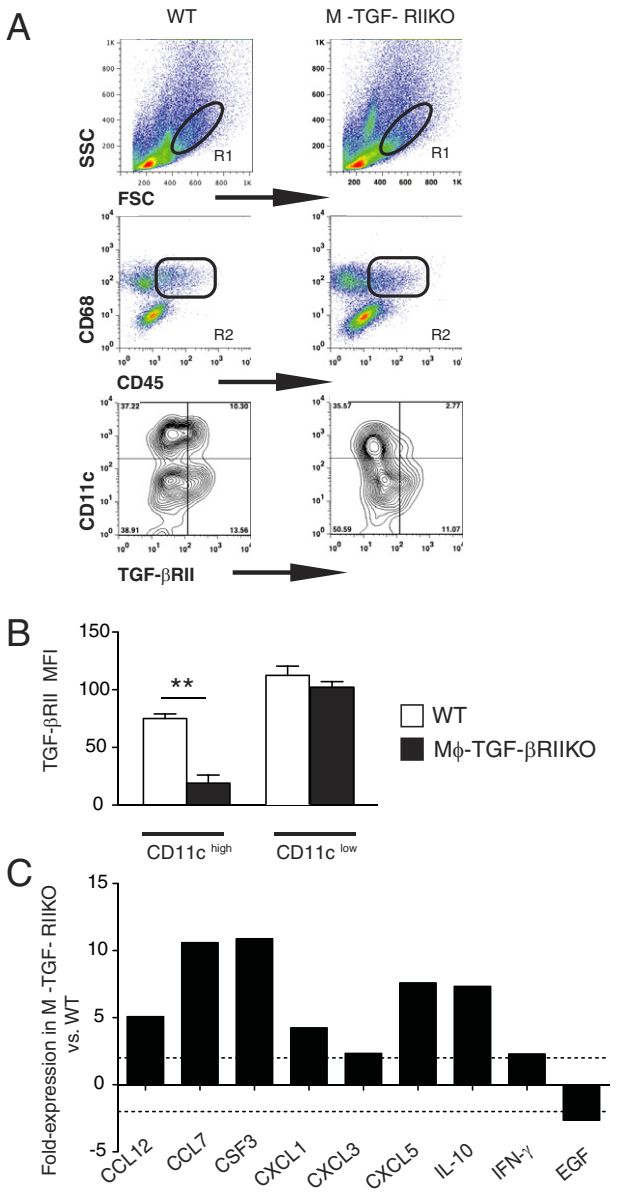

Figure 1. Naïve Mϕ-TGF-βRIIKO mice have reduced TGF-βRII expression on lung macrophages and develop pulmonary inflammation at baseline. **A:** Flow cytometry gating strategy for the identification of TGF-βRII expression on CD11c-positive cell populations in whole lung digests of naïve wild-type (WT) and Mϕ-TGF-βRIIKO mice. $FSC^{high}SSC^{low}$ cells (R1) that coexpressed CD45 and CD68 (R2) were evaluated for surface expression of CD11c and TGF-βRII. In the contour plots, the percentage of positive cells is indicated in each quadrant. **B:** Mean fluorescence intensity (MFI) for TGF-βRII on the $CD11c^{low}$ and $CD11c^{high}$ populations. **C:** Results of a quantitative RT-PCR-based wound-healing array performed on whole lung tissues from naïve WT and Mϕ-TGF-βRIIKO strains. Data are expressed as means ± SEM (**B**) or from pooled samples representative of two independent experiments (**C**). $^{**}P < 0.01$. $n = 4$ mice (**A** and **B**); $n = 2$ or 3 mice (**C**) per group.

had reduced TGF-βRII expression accompanied by marked dysregulation of inflammatory/tissue repair genes.

Macrophages from Mϕ-TGF-βRIIKO Mice Fail to Suppress T-Cell Activation

TGF-β inhibits leukocyte activation and proliferation through diverse mechanisms, one example of which is through promoting a suppressive phenotype in macrophages.[30–32] To evaluate suppressor macrophage activity, BMDMs were generated from both mouse strains and were used as the source of antigen presenting cells (APC) in a coculture system with naïve antigen-specific $CD4^+$ T cells.[12] BMDMs were exposed to medium only (mock treatment), treated with rTGF-β (10 ng/mL; TGF-β treatment), ovalbumin peptide 323–339 (1 mg/mL; OVA treatment), or rTGF-β and OVA-peptide (OVA+TGF-β treatment) for 16 hours, then were washed and cocultured with $CD4^+$ T cells purified from ovalbumin-specific TCR transgenic mice (OTII) at a 5:1 ratio (Mϕ:$CD4^+$ T cells) for 96 hours. Flow cytometry was used to evaluate the TCR-β $CD4^+$ cells (Figure 2A) for activation status and relative

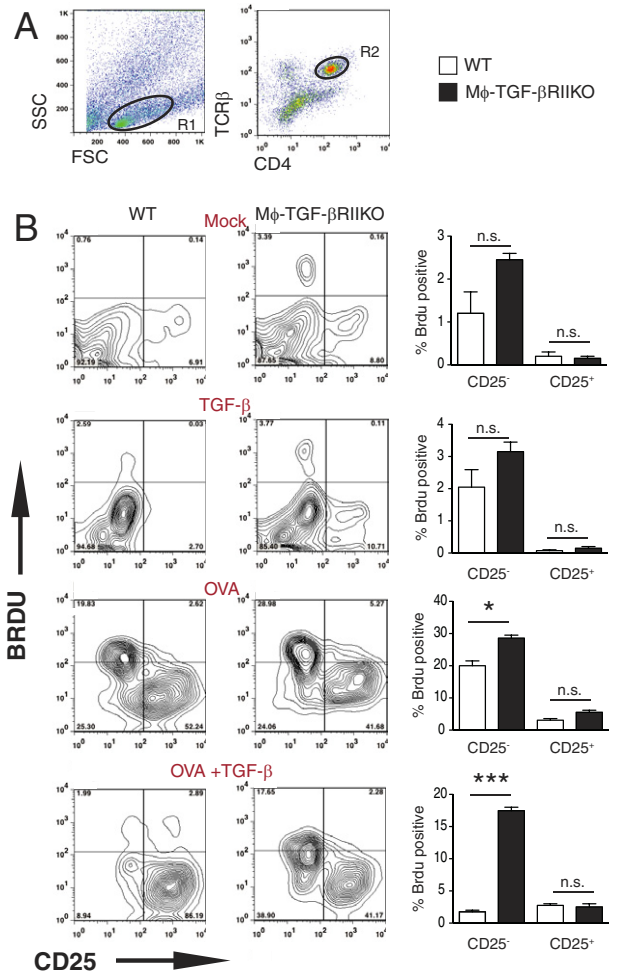

Figure 2. Bone marrow-derived macrophages (BMDMs) from Mϕ-TGF-βRIIKO mice lack TGF-β–mediated suppression of antigen-specific T cell activation. **A:** Flow cytometry gating strategy for the identification of ovalbumin-specific TCR transgenic $CD4^+$ lymphocytes (OTII) after coculture with BMDMs from WT or Mϕ-TGF-βRIIKO mice via coexpression of TCR-β and CD4. **B:** Representative contour plots of gated $CD4^+$ T cells show the level of BrdU incorporation and cell surface expression of CD25 (IL-2Rα) at 96 hours. In the contour plots, the percentage of positive cells is indicated in each quadrant in contour plots; in the bar graphs, the percentage of BrdU-positive cells in the $CD25^-$ or $CD25^+$ gate is shown. APC-$CD4^+$ T-cell cocultures were administered medium only (Mock), 20 ng/mL recombinant murine TGF-β (TGF-β), 1 mg/mL OVA peptide (OVA), or TGF-β and OVA peptide. Data are expressed as means ± SEM of quadruplicate wells and are representative of two independent experiments. $^*P < 0.05$; $^{***}P < 0.001$. $n = 4$ mice per group. n.s., not significant.

amount of DNA synthesis via detection of CD25 (IL-2Rα) and BrdU incorporation, respectively. Although the baseline BrdU incorporation in the CD25-negative population was moderately increased in Mϕ-TGF-βRIIKO APC-T cell cocultures, compared with the WT, this increase became significant after the administration of OVA. Strikingly, antigen-specific BrdU incorporation in cocultures of $CD4^+$ T cells and OVA peptide-pulsed WT macrophages was abrogated in the presence of TGF-β treatment (1.9%), whereas $CD4^+$ T cells in Mϕ-TGF-βRIIKO APC-T cell cocultures maintained a significant level of BrdU incorporation (17.6%), despite pre-exposure to TGF-β–treated macrophages (Figure 2B). These results suggest that BMDMs from Mϕ-TGF-βRIIKO mice displayed a marked impairment of TGF-β–mediated suppressor macrophage function.

Mice That Lack TGF-β Responsive Myeloid Cells Generate Enhanced Type 2 Immune Responses after N. brasiliensis *Infection*

Helminths can elicit TGF-β production in their hosts as part of an immune evasion strategy.[33,34] To determine whether TGF-β–dependent effects on myeloid cells serve an important role, WT and Mϕ-TGF-βRIIKO mice were subcutaneously infected with 500 *N. brasiliensis* infective-stage larvae, and the numbers of parasite eggs produced in the feces were monitored between 6 and 10 days after infection. Worm egg production terminated more rapidly in Mϕ-TGF-βRIIKO mice than in WT mice at day 8 and 9 after infection (Figure 3A). Adult worm numbers at day 9 after infection were moderately reduced in Mϕ-TGF-βRIIKO mice, compared with WT mice (data not shown).

Next, type 2 cytokine and antibody production were measured to determine whether TGF-β effects on myeloid cells regulate the immune response to *N. brasiliensis* infection.[22] Total serum levels of IgE were increased in WT mice at 14 days after infection, but were significantly higher in Mϕ-TGF-βRIIKO mice (Figure 3B). The *in vivo* cytokine capture assay was used to evaluate IL-4, IL-10, and IFN-γ levels in the sera of naïve and infected WT and Mϕ-TGF-βRIIKO mice. Mice were injected with biotin-conjugated antibody on day 8, and then were bled on day 9 to determine the amount of cytokine produced in the systemic circulation. Congruent with *N. brasiliensis* infection-induced IgE levels, the production of IL-4 was greater in Mϕ-TGF-βRIIKO mice, compared with the WT (Figure 3C). In contrast, IFN-γ and IL-10 levels were low in both strains and were not significantly different (Figure 3C).

Given that migratory *N. brasiliensis* larvae cause lung injury and marked pulmonary type 2 inflammation,[35] BALF was evaluated for cytokine production. Notably, Mϕ-TGF-βRIIKO mice produced greater amounts of TGF-β (Figure 3D) and IL-13 (Figure 3E) than WT littermates at 9 days after infection. Taken together, these data indicate that mice lacking TGF-β–responsive myeloid cells develop more robust type 2 immunity than do WT mice after *N. brasiliensis* infection.

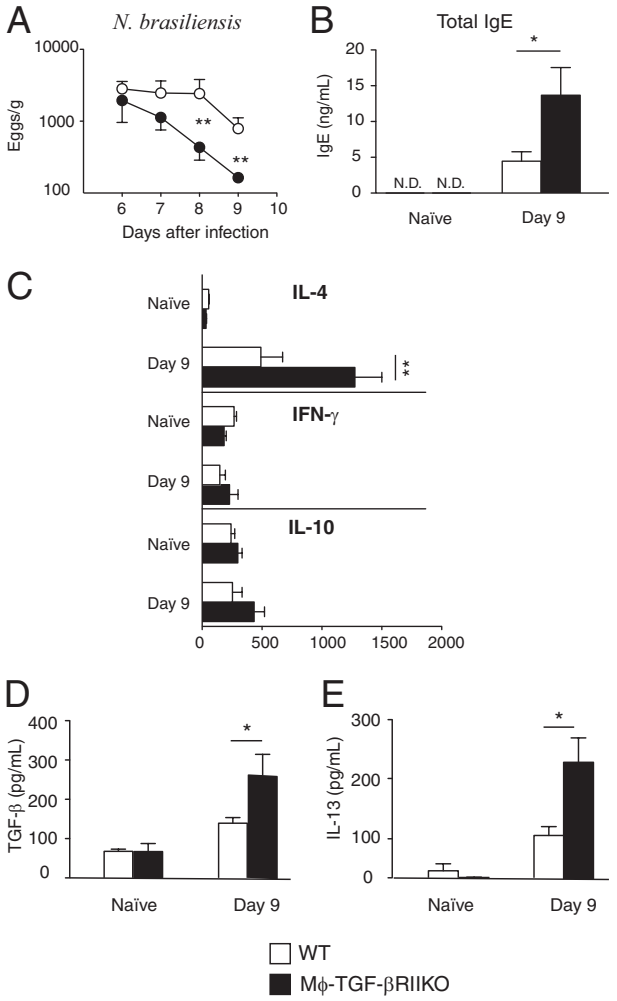

Figure 3. Mϕ-TGF-βRIIKO mice generate enhanced type 2 immunity against the hookworm *N. brasiliensis*. **A:** WT mice (open symbols) and Mϕ-TGF-βRIIKO mice (closed symbols) were subcutaneously infected with 750 *N. brasiliensis* infective-stage larvae (L3) and were evaluated for fecal egg production from adult worms in the intestinal lumen. **B:** Untreated (naïve) or infected mice from both strains were evaluated for total serum levels of IgE. **C:** Systemic levels of IL-4, IFN-γ and IL-10 were determined by *in vivo* cytokine capture assay. **D** and **E:** Levels in BALF of TGF-β (**D**) and IL-13 (**E**), as determined by sandwich ELISA. Data are expressed as means ± SEM and are representative of four independent experiments. $^*P < 0.05$; $^{**}P < 0.01$. $n = 6$ to 8 mice per group. N.D., not detected.

Mϕ-TGF-βRIIKO Mice Develop Enhanced Emphysematous Pathology after N. brasiliensis *Infection*

N. brasiliensis L_3 larvae cause severe hemorrhagic lung injury within the first three days of primary inoculation. Resolution of tissue damage occurs over months and is marked by the accumulation of AAMϕ, excess collagen deposition, and progressive development of lung hyperresponsiveness.[20,36,37] We asked whether TGF-β effects on myeloid cells are important for the regulation of tissue repair and pulmonary function. To this end, cohorts of WT and Mϕ-TGF-βRIIKO mice were evaluated longitudinally by whole-body plethysmography after infection, to monitor the progressive changes in breathing dynamics of unrestrained animals. Results showed that, before cho-

linergic stimulation, the infected Mϕ-TGF-βRIIKO mice developed a progressive increase in respiration time in the weeks after parasite clearance, compared with their WT cohorts (Figure 4A). Using this approach, respiration time RT is defined as the length of time required to expire 65% of total lung volume. Comparison of the methacholine-induced enhanced pause (Penh) response between strains revealed that WT mice developed a progressive and significant increase in Penh, whereas Penh values in Mϕ-TGF-βRIIKO mice did not increase over time (Figure 4B).

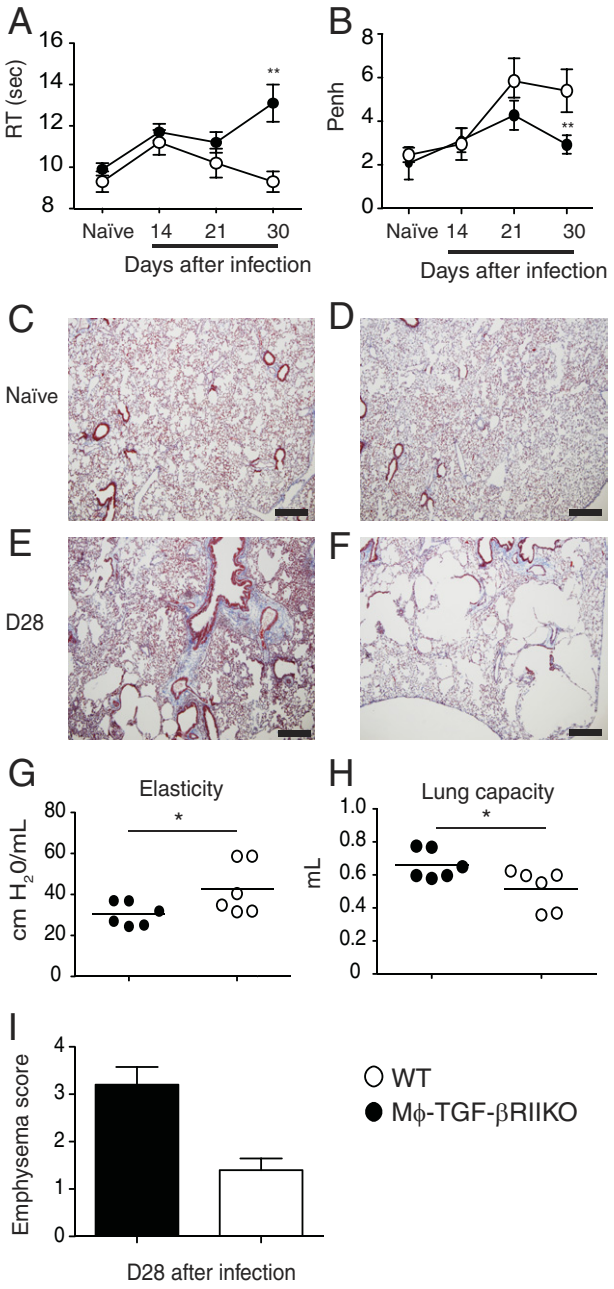

Figure 4. Mϕ-TGF-βRIIKO mice rapidly develop emphysema-like pathology after hookworm infection. **A** and **B:** Whole-body plethysmography via the Buxco system was performed on cohorts of naïve and *N. brasiliensis*-infected mice at the indicated time points for evaluation of baseline respiration time (RT) (**A**) and changes in breathing patterns (the enhanced pause response, Penh) (**B**) during the breathing cycle after methacholine-induced bronchoconstriction (25 mg/mL). **C–F:** Representative histological sections of lung tissues from WT mice (**C** and **E**) and Mϕ-TGF-βRIIKO mice (**D** and **F**). Masson's trichrome staining was used to demonstrate areas of collagen deposition (blue). **G–I:** A flexiVent system was used to evaluate lung elasticity (**G**) and total lung capacity (**H**) in both strains at day 28 after infection, and clinical score for emphysematous pathology was determined (**I**). Data are representative of three independent experiments (**A** and **B**). Data are expressed as means ± SEM. $^{*}P < 0.05$, $^{**}P < 0.01$. $n = 6$ to 8 mice (**A** and **B**); $n = 6$ mice (**G** and **H**); $n = 4$ mice (**I**) per group. Scale bar = 100 μm.

Compared with the WT, Mϕ-TGF-βRIIKO mice produced higher levels of the profibrotic cytokines IL-13 and TGF-β in BALF at 9 days after infection. We therefore subjected paraffin-embedded sections of lung tissue to Masson's trichrome stain, to evaluate whether there were differences in collagen accumulation between strains. Although there were no obvious differences in lung architecture between naïve mice of either strain (Figure 4, C and D), by 28 days after infection both strains showed some evidence of moderate collagen accumulation, indicative of subepithelial cell fibrosis (Figure 4, E and F). Notably, the alveolar structure in Mϕ-TGF-βRIIKO mice was markedly defective, with large areas of irregular bronchiolar dilation that resembled emphysematous bullae and perivascular edema (Figure 4F). In contrast, WT mice had moderate alveolar emphysema, with mildly thickened lung interstitium and infiltrates of small lymphocytes and histiocytes.

In addition, a flexiVent apparatus was used to measure airway mechanics in the two strains. Interestingly, there were no differences between strains in methacholine-induced airway resistance; however, infected Mϕ-TGF-βRIIKO mice had significantly reduced lung elasticity (Figure 4G) and significantly greater total lung capacity (Figure 4H), compared with WT mice at 28 days after infection. Mϕ-TGF-βRIIKO mice had more emphysematous bullae, compared with WT mice at 28 days after infection, as determined by our clinical scoring system (Figure 4I). Taken together, these data show that hookworm infection-induced lung injury in Mϕ-TGF-βRIIKO mice results in more rapid emphysematous lung pathology than in WT mice.[20]

TGF-β Responsiveness in Myeloid Cells Is Not Required for Alternative Macrophage Activation or Infection-Induced Lung Fibrosis

Given the progressive accumulation of AAMϕ and lung fibrosis during the chronic repair phase of *N. brasiliensis* infection,[36] we evaluated whether TGF-β–responsive myeloid cells were responsible for AAMϕ gene expression or profibrotic cytokines release during the chronic stages of repair. Surprisingly, there were no differences between strains in lung hydroxyproline content at 28 days after infection (Figure 5A), but fibronectin levels were significantly higher in Mϕ-TGF-βRIIKO mice, compared with WT mice (Figure 5B). BALF levels of TGF-β and IL-13 at day 28 after infection did not differ between strains (Figure 5, C and D).

Whole lung tissue was analyzed for the expression of *Arg1* and *Retnla* genes, which are strongly associated with AAMϕ and the wound-healing response.[38] There were no differences in *Retnla* expression, but significantly increased *Arg1* expression was noted in the lungs of

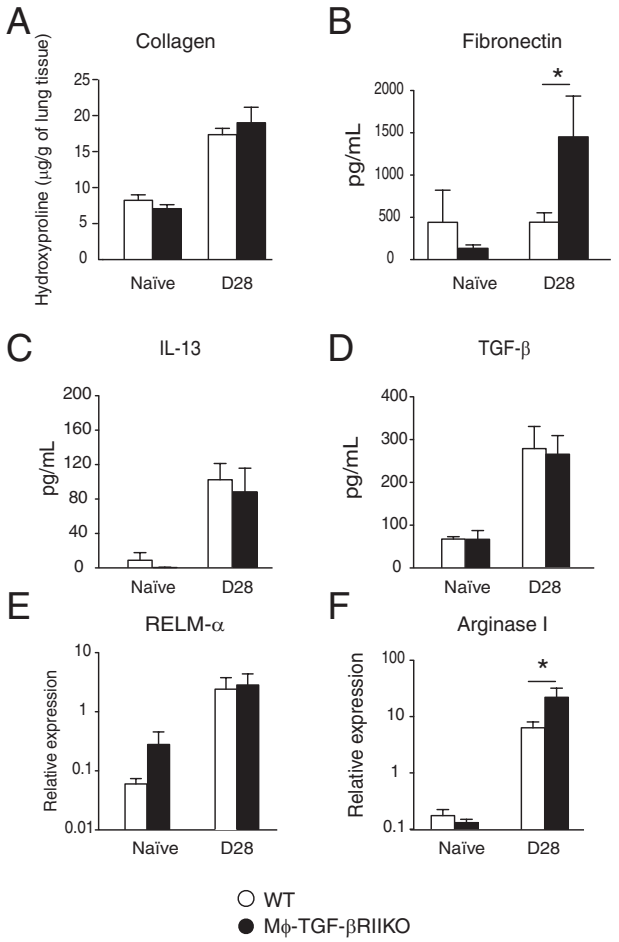

Figure 5. Mϕ-TGF-βRIIKO mice up-regulate fibronectin production and arginase I expression during the chronic repair phase of hookworm-mediated lung injury. WT and Mϕ-TGF-βRIIKO mice were subcutaneously infected with 750 *N. brasiliensis* infective-stage larvae (L3). Whole lung tissues of naïve and infected mice at 28 days after infection were evaluated for hydroxyproline levels of collagen in individual lobes of lung tissue (**A**), for BALF levels of fibronectin (**B**), IL-13 (**C**), and TGF-β1 (**D**), and for mRNA expression levels of RELMα (**E**) and arginase I (**F**). Data are representative of three independent experiments. Data are expressed as means ± SEM. $^*P < 0.05$. $n = 6$ to 8 mice per group.

Mϕ-TGF-βRIIKO mice, compared with WT mice at day 28 after infection (Figure 5, E and F). Taken together, these data suggest that TGF-β–dependent effects on myeloid cells are not critical for hookworm-induced lung fibrosis, profibrotic cytokine production, or the expression of genes associated with AAMϕ.

N. Brasiliensis-*Induced Lung Injury in Mϕ-TGF-βRIIKO Mice Results in a Marked Dysregulation of Matrix Metalloprotease Activity*

Mϕ-TGF-βRIIKO mice exhibited a marked dysregulation of lung physiology after hookworm infection.[39–41] We therefore evaluated a wide array of inflammation and wound-healing genes, again using the quantitative RT-PCR-based cDNA array, to determine whether TGF-β effects on myeloid cells regulate chronic lung repair more broadly. Comparison between strains at 28 days after infection revealed multiple genes that were either up- or down-regulated more than twofold, compared with WT controls (Figure 6A). Similar to differences between strains before infection, Mϕ-TGF-βRIIKO mice expressed higher levels of proinflammatory chemokines and chemokines genes (*Ccl12*, *Ccl7*, *Csf3*, *Cxcl1*, *Cxcl3*, *Cxcl5*, and *Tnf*), compared with WT mice, but also the canonical anti-inflammatory cytokine gene *Il10*.

There was evidence for broad dysregulation of MMP activity, shown by increased expression of tissue inhibitor of matrix metalloprotease 1 (*Timp1*), and increased expression of several matrix metalloprotease genes (including *Mmp1a* and *Mmp2*) in Mϕ-TGF-βRIIKO mice, compared with WT mice (Figure 6A). Conversely, Mϕ-TGF-βRIIKO mice had a notable decrease in expression of *Egfr* and *Mmp7* (Figure 6A). Although *N. brasiliensis*-damaged lung tissue has been demonstrated to express elevated *Mmp12* levels, this gene was not part of the array and could not be assessed.

Given the transcriptional dysregulation of several MMP genes and *Timp1*, the overall MMP enzymatic activity in BALF was determined. The Mϕ-TGF-βRIIKO mice had moderately increased baseline activity, but a significantly greater infection-induced MMP activity, than WT mice at day 28 (Figure 6B). Thus, TGF-β–dependent regulation of myeloid cell function serves a critical *in vivo* role for suppression of cytokine/chemokine production and MMP activity in lung tissues after *N. brasiliensis* infection.

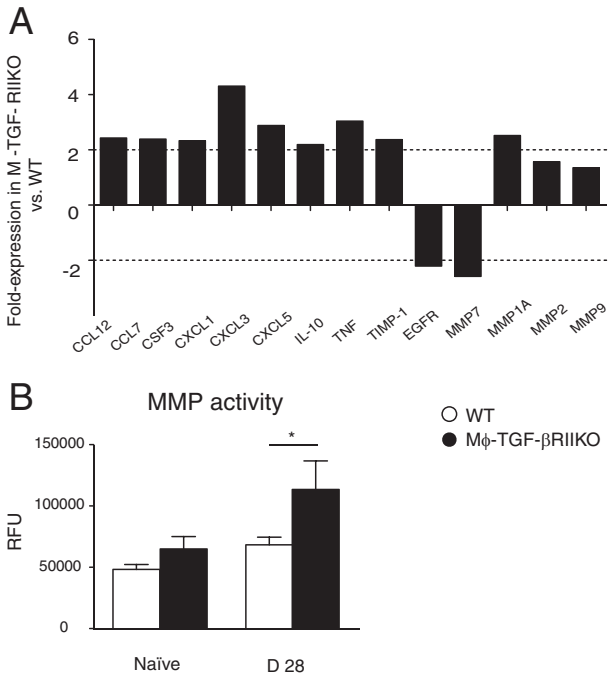

Figure 6. Chronic lung repair in Mϕ-TGF-βRIIKO mice is marked by dysregulated MMP production. **A:** Results of a quantitative RT-PCR-based array for wound-healing genes performed on whole lung tissue from WT and Mϕ-TGF-βRIIKO strains at 28 days after infection. **B:** Total matrix metalloprotease (MMP) activity in BALF of naïve and infected WT and Mϕ-TGF-βRIIKO strains at 28 days after infection. Data are representative of two independent experiments. Data represent pooled samples (**A**) or are expressed as means ± SEM (**B**). $^*P < 0.05$. $n = 2$ or 3 mice (**A**); $n = 6$ to 8 mice (**B**) per group.

Discussion

The present study demonstrated that TGF-β–dependent effects on myeloid lineage cells regulate type 2 responses and pulmonary repair mechanisms during *N. brasiliensis* infection. Given that infected Mϕ-TGF-βRIIKO mice produced greater amounts of type 2 cytokines (IL-4 and IL-13) and greater emphysematous pathology than WT mice, our data suggest that TGF-β negatively regulates host protection against hookworms, but critically regulates infection-induced tissue damage. Indeed, TGF-β instructed myeloid cells to restrict the tissue levels of inflammatory cytokine/chemokines and MMPs in the lung, which demonstrates a previously unrecognized mechanism for TGF-β–responsive myeloid cells in the host-protective mechanisms engaged in worm-infected hosts.

Many pathogens elicit host-derived TGF-β production, but evidence that parasitic worms encode TGF-β–like molecules emphasizes the importance of this cytokine in the context of helminth infection.[15] Demonstration that mice lacking TGF-β–responsive myeloid cells develop enhanced immunity and excessive immunopathology in response to *N. brasiliensis* infection supports the notion that TGF-β promotes chronic worm infestations. Indeed, TGF-β neutralization results in the rapid development of host immunity and worm clearance in otherwise chronically infected hosts.[42] TGF-β production during helminth infections can suppress inflammation in distinct organ environments.[43] In addition to its role in lymphocyte regulation, we demonstrate an important role for TGF-β specifically in myeloid cell function. Indeed, BMDMs exposed to TGF-β suppressed antigen-specific T-cell proliferation, whereas those derived from Mϕ-TGF-βRIIKO mice failed to do so in our *in vitro* coculture system. $CD4^+$ T cells isolated from *N. brasiliensis*-infected Mϕ-TGF-βRIIKO mice also showed greater degree of BrdU incorporation and CD25 expression, compared with similarly infected WT mice (data not shown). Although our data show an important role for this mechanism in the context of hookworm infection, it is likely that TGF-β responsiveness in myeloid cells promotes chronic infections with other helminths.

Mϕ-TGF-βRIIKO mice generated increased levels of IgE and type 2 cytokines after *N. brasiliensis* infection, compared with WT controls. It is likely that increased type 2 responses were responsible for the enhanced immunity. Although this has not been formally demonstrated, the underlying mechanism for accelerated type 2 immunity could be enhanced production of macrophage-derived IL-33, because we have demonstrated that TGF-β is a negative regulator of IL-33 production in tissue macrophages.[44] Indeed, IL-33 is a strong inducer of type 2 inflammation and drives the expulsion of the gastrointestinal helminth *Trichuris muris*.[45,46] IL-33 may also drive the differentiation of AAMϕ,[47] which promotes immunity against parasitic helminths. Although it remains unclear whether macrophage-derived IL-33 was indeed responsible for the enhanced immunity against *N. brasiliensis*, our data show that TGF-β effects on myeloid cells antagonizes the expression of arginase I, a central effector molecule expressed by AAMϕ. Given the broad implication of AAMϕ as key players in mucosal immunity, it will be important to evaluate whether Mϕ-TGF-βRIIKO mice have altered susceptibility to other types of pathogens.[12,38]

Curiously, naïve Mϕ-TGF-βRIIKO mice demonstrated a moderate increase of lung inflammation, as shown by increased numbers of SSC^{high} cells (characteristic of granulocytes). Given that TGF-β suppresses neutrophil effector function,[48] we cannot rule out the possibility that lack of neutrophil responsiveness to TGF-β in the Mϕ-TGF-βRIIKO strain partially explains this phenotype. Nonetheless, the increased baseline inflammation was associated with increased expression of myeloid-specific chemokine genes such as *Ccl12*, *Ccl7*, *Cxcl1*, *Cxcl3*, and *Cxcl5*,[49,50] as well as a marked reduction in wound-healing genes such as *Egf*, which regulates mucosal barrier integrity. Furthermore, our observation that Mϕ-TGF-βRIIKO mice had dysregulated MMP gene expression at baseline and after *N. brasiliensis* infection is consistent with the established role for TGF-β in the negative regulation of MMPs from a variety of cellular sources.[10,51]

Importantly, TGF-β responsiveness in myeloid cell function helps to maintain pulmonary function after *N. brasiliensis* infection-induced lung injury. Loss of this pathway in Mϕ-TGF-βRIIKO mice resulted in phenotypical characteristics of chronic obstructive pulmonary disease (COPD)/emphysema, including loss of tissue elasticity, increased total lung capacity, and destruction of alveolar structure.[52,53] Two methods were used to evaluate lung mechanics as surrogate markers for the quality of pulmonary repair in the weeks after parasite expulsion. First, we used the Buxco system, which has been widely used for evaluation of the airflow changes that characterize allergic asthma, including smooth muscle hypercontractility, mucus accumulation, and inflammatory cell recruitment. However, it has become increasingly appreciated that this method of evaluating lung function in mice does not accurately reflect airway hyper-responsiveness normally associated with allergic asthma, because noninvasive plethysmography records only the overall changes in air pressure during the breathing cycle.[54] This does not allow Penh (enhanced pause) to distinguish between airflow obstruction of the upper or lower airway.[54] Thus, our data showing that the infection-induced progression of Penh values in Mϕ-TGF-βRIIKO mice were markedly less than those in WT mice reflects only the larger areas of lung tissue that remained unrepaired in the former, compared with the latter. Thus, methacholine-induced bronchoconstriction is markedly less pronounced in Mϕ-TGF-βRIIKO mice because of an overall increase in total lung capacity. Indeed, the respiration time RT was significantly longer in Mϕ-TGF-βRIIKO mice than in WT mice.

We also used a flexiVent system, which requires intratracheal intubation to specifically interrogate lung mechanics in the lower airway. Using this method, we found no difference between strains in methacholine-induced airway resistance (data not shown), but a significant reduction of lung tissue elasticity and increase in total lung capacity in Mϕ-TGF-βRIIKO mice, compared with WT littermates. Thus, our data are consistent with a more

rapid progression of an emphysema-like disease in hookworm-infected mice that lack TGF-β–responsive myeloid cells. The central pathological feature of emphysema is the collapse of alveolar septae, which results in abnormally large airspaces.[55–57] These large cavities that result from septal rupture are termed bullae, a pathological feature that was readily apparent in the lung tissues of Mϕ-TGF-βRIIKO mice by 21 to 28 days after infection. The current consensus is that COPD/emphysema is precipitated by excess production of proteolytic enzymes, such as neutrophil elastase or MMPs.[53] Moreover, humans with genetic defects in protease neutralizing enzymes, such as α1-anti-trypsin deficiency, show an increased risk for the development of emphysema.[58] Importantly, defects in TGF-βRII signaling have been implicated in emphysema/COPD pathogenesis.[59,60] TGF-β may directly regulate MMP activity through inducing TIMP genes.[51,61] There was an overall increase of total MMP activity in BALF of Mϕ-TGF-βRIIKO mice at 28 days after infection, compared with WT mice. This is consistent with increased expression of MMP12 from alveolar macrophages after *N. brasiliensis* infection. However, MMP12-deficient mice are not protected from hookworm-induced emphysema.[20] Thus, it remains unclear how TGF-β effects on myeloid cells regulate the progression of emphysema. In conclusion, we have demonstrated that the *in vivo* effects of TGF-β on myeloid phagocytes suppress host immunity during parasitic worm infection and limit the excessive tissue injury that culminates in chronic lung disease.

Acknowledgments

We thank Dr. Fred D. Finkelman and the CCHMC Immunobiology program staff for assistance in the completion of this article.

References

1. Massagué J, Blain SW, Lo RS: TGFbeta signaling in growth control, cancer, and heritable disorders. Cell 2000, 103:295–309
2. Thomas DA, Massagué J: TGF-beta directly targets cytotoxic T cell functions during tumor evasion of immune surveillance. Cancer Cell 2005, 8:369–380
3. Hall A, Massagué J: Cell regulation. Curr Opin Cell Biol 2008, 20:117–118
4. Shull MM, Ormsby I, Kier AB, Pawlowski S, Diebold RJ, Yin M, Allen R, Sidman C, Proetzel G, Calvin D, Annunziata N, Doetschman T: Targeted disruption of the mouse transforming growth factor-beta 1 gene results in multifocal inflammatory disease. Nature 1992, 359: 693–699
5. Kriegel MA, Li MO, Sanjabi S, Wan YY, Flavell RA: Transforming growth factor-beta: recent advances on its role in immune tolerance. Curr Rheumatol Rep 2006, 8:138–144
6. Li MO, Sanjabi S, Flavell RA: Transforming growth factor-beta controls development, homeostasis, and tolerance of T cells by regulatory T cell-dependent and -independent mechanisms. Immunity 2006, 25: 455–471
7. Li MO, Wan YY, Sanjabi S, Robertson AK, Flavell RA: Transforming growth factor-beta regulation of immune responses. Annu Rev Immunol 2006, 24:99–146
8. Shah M, Revis D, Herrick S, Baillie R, Thorgeirson S, Ferguson M, Roberts A: Role of elevated plasma transforming growth factor-beta1 levels in wound healing. Am J Pathol 1999, 154:1115–1124
9. Gratchev A, Kzhyshkowska J, Kannookadan S, Ochsenreiter M, Popova A, Yu X, Mamidi S, Stonehouse-Usselmann E, Muller-Molinet I, Gooi L, Goerdt S: Activation of a TGF-beta-specific multistep gene expression program in mature macrophages requires glucocorticoid-mediated surface expression of TGF-beta receptor II. J Immunol 2008, 180:6553–6565
10. Feinberg MW, Jain MK, Werner F, Sibinga NE, Wiesel P, Wang H, Topper JN, Perrella MA, Lee ME: Transforming growth factor-beta 1 inhibits cytokine-mediated induction of human metalloelastase in macrophages. J Biol Chem 2000, 275:25766–25773
11. Werner F, Jain MK, Feinberg MW, Sibinga NE, Pellacani A, Wiesel P, Chin MT, Topper JN, Perrella MA, Lee ME: Transforming growth factor-beta 1 inhibition of macrophage activation is mediated via Smad3. J Biol Chem 2000, 275:36653–36658
12. Herbert DR, Orekov T, Roloson A, Ilies M, Perkins C, O'Brien W, Cederbaum S, Christianson DW, Zimmermann N, Rothenberg ME, Finkelman FD: Arginase I suppresses IL-12/IL-23p40-driven intestinal inflammation during acute schistosomiasis. J Immunol 2010, 184: 6438–6446
13. Zhao A, Urban JF Jr, Anthony RM, Sun R, Stiltz J, van Rooijen N, Wynn TA, Gause WC, Shea-Donohue T: Th2 cytokine-induced alterations in intestinal smooth muscle function depend on alternatively activated macrophages. Gastroenterology 2008, 135:217–225.e1
14. Anthony RM, Urban JF Jr, Alem F, Hamed HA, Rozo CT, Boucher JL, Van Rooijen N, Gause WC: Memory TH2 cells induce alternatively activated macrophages to mediate protection against nematode parasites. Nat Med 2006, 12:955–960
15. Grainger JR, Smith KA, Hewitson JP, McSorley HJ, Harcus Y, Filbey KJ, Finney CA, Greenwood EJ, Knox DP, Wilson MS, Belkaid Y, Rudensky AY, Maizels RM: Helminth secretions induce de novo T cell Foxp3 expression and regulatory function through the TGF-beta pathway. J Exp Med 2010, 207:2331–2341
16. Pesce JT, Ramalingam TR, Mentink-Kane MM, Wilson MS, El Kasmi KC, Smith AM, Thompson RW, Cheever AW, Murray PJ, Wynn TA: Arginase-1-expressing macrophages suppress Th2 cytokine-driven inflammation and fibrosis. PLoS Pathog 2009, 5:e1000371
17. Pesce JT, Ramalingam TR, Wilson MS, Mentink-Kane MM, Thompson RW, Cheever AW, Urban JF Jr, Wynn TA: Retnla (relmalpha/fizz1) suppresses helminth-induced Th2-type immunity. PLoS Pathog 2009, 5:e1000393
18. Coyle AJ, Kohler G, Tsuyuki S, Brombacher F, Kopf M: Eosinophils are not required to induce airway hyperresponsiveness after nematode infection. Eur J Immunol 1998, 28:2640–2647
19. Wills-Karp M, Luyimbazi J, Xu X, Schofield B, Neben TY, Karp CL, Donaldson DD: Interleukin-13: central mediator of allergic asthma. Science 1998, 282:2258–2261
20. Marsland BJ, Kurrer M, Reissmann R, Harris NL, Kopf M: Nippostrongylus brasiliensis infection leads to the development of emphysema associated with the induction of alternatively activated macrophages. Eur J Immunol 2008, 38:479–488
21. Chytil A, Magnuson MA, Wright CV, Moses HL: Conditional inactivation of the TGF-beta type II receptor using Cre: Lox. Genesis 2002, 32:73–75
22. Herbert DR, Yang JQ, Hogan SP, Groschwitz K, Khodoun M, Munitz A, Orekov T, Perkins C, Wang Q, Brombacher F, Urban JF Jr, Rothenberg ME, Finkelman FD: Intestinal epithelial cell secretion of RELM-b protects against gastrointestinal worm infection. J Exp Med 2009, 206:2947–2957
23. Herbert DR, Hölscher C, Mohrs M, Arendse B, Schwegmann A, Radwanska M, Leeto M, Kirsch R, Hall P, Mossmann H, Claussen B, Förster I, Brombacher F: Alternative macrophage activation is essential for survival during schistosomiasis and downmodulates T helper 1 responses and immunopathology [Erratum appeared in Immunity 2004, 21:455]. Immunity 2004, 20:623–635
24. Finkelman FD, Morris SC: Development of an assay to measure in vivo cytokine production in the mouse. Int Immunol 1999, 11:1811–1818
25. Salazar E, Knowles JH. An analysis of pressure-volume characteristics of the lungs. J Appl Physiol 1964, 19:97–104
26. Frugier T, Koishi K, Matthaei KI, McLennan IS: Transgenic mice carrying a tetracycline-inducible, truncated transforming growth factor beta receptor (TbetaRII). Genesis 2005, 42:1–5
27. Laouar Y, Sutterwala FS, Gorelik L, Flavell RA: Transforming growth factor-beta controls T helper type 1 cell development through regu-

lation of natural killer cell interferon-gamma. Nat Immunol 2005, 6:600–607
28. Plantinga M, Hammad H, Lambrecht BN: Origin and functional specializations of DC subsets in the lung. Eur J Immunol 2010, 40:2112–2118
29. Hammad H, Plantinga M, Deswarte K, Pouliot P, Willart MA, Kool M, Muskens F, Lambrecht BN: Inflammatory dendritic cells–not basophils–are necessary and sufficient for induction of Th2 immunity to inhaled house dust mite allergen. J Exp Med 2010, 207:2097–2111
30. Walsh KP, Brady MT, Finlay CM, Boon L, Mills KH: Infection with a helminth parasite attenuates autoimmunity through TGF-beta-mediated suppression of Th17 and Th1 responses. J Immunol 2009, 183:1577–1586
31. Taylor MD, Harris A, Nair MG, Maizels RM, Allen JE: F4/80+ alternatively activated macrophages control $CD4^+$ T cell hyporesponsiveness at sites peripheral to filarial infection. J Immunol 2006, 176: 6918–6927
32. Mantovani A, Sozzani S, Locati M, Allavena P, Sica A: Macrophage polarization: tumor-associated macrophages as a paradigm for polarized M2 mononuclear phagocytes. Trends Immunol 2002, 23:549–555
33. Maizels RM, Balic A, Gomez-Escobar N, Nair M, Taylor MD, Allen JE: Helminth parasites–masters of regulation. Immunol Rev 2004, 201: 89–116
34. Reyes JL, Terrazas LI: The divergent roles of alternatively activated macrophages in helminthic infections. Parasite Immunol 2007, 29: 609–619
35. Chen F, Liu Z, Wu W, Rozo C, Bowdridge S, Millman A, Van Rooijen N, Urban JF Jr, Wynn TA, Gause WC: An essential role for TH2-type responses in limiting acute tissue damage during experimental helminth infection. Nat Med 2012, 18:260–266
36. Reece JJ, Siracusa MC, Southard TL, Brayton CF, Urban JF Jr, Scott AL: Hookworm-induced persistent changes to the immunological environment of the lung. Infect Immun 2008, 76:3511–3524
37. Siracusa MC, Reece JJ, Urban JF Jr, Scott AL: Dynamics of lung macrophage activation in response to helminth infection. J Leukoc Biol 2008, 84:1422–1433
38. Gordon S, Martinez FO: Alternative activation of macrophages: mechanism and functions. Immunity 2010, 32:593–604
39. Barron L, Wynn TA: Fibrosis is regulated by Th2 and Th17 responses and by dynamic interactions between fibroblasts and macrophages. Am J Physiol Gastrointest Liver Physiol 2011, 300:G723–G728
40. Wynn TA, Barron L: Macrophages: master regulators of inflammation and fibrosis. Semin Liver Dis 2010, 30:245–257
41. Wynn TA: Integrating mechanisms of pulmonary fibrosis. J Exp Med 2011, 208:1339–1350
42. Taylor MD, LeGoff L, Harris A, Malone E, Allen JE, Maizels RM: Removal of regulatory T cell activity reverses hyporesponsiveness and leads to filarial parasite clearance in vivo. J Immunol 2005, 174:4924–4933
43. Wilson MS, Taylor MD, Balic A, Finney CA, Lamb JR, Maizels RM: Suppression of allergic airway inflammation by helminth-induced regulatory T cells. J Exp Med 2005, 202:1199–1212
44. Rani R, Smulian AG, Greaves DR, Hogan SP, Herbert DR: TGF-beta limits IL-33 production and promotes the resolution of colitis through regulation of macrophage function. Eur J Immunol 2011, 41:2000–2009
45. Humphreys NE, Xu D, Hepworth MR, Liew FY, Grencis RK: IL-33, a potent inducer of adaptive immunity to intestinal nematodes. J Immunol 2008, 180:2443–2449
46. Schmitz J, Owyang A, Oldham E, Song Y, Murphy E, McClanahan TK, Zurawski G, Moshrefi M, Qin J, Li X, Gorman DM, Bazan JF, Kastelein RA: IL-33, an interleukin-1-like cytokine that signals via the IL-1 receptor-related protein ST2 and induces T helper type 2-associated cytokines. Immunity 2005, 23:479–490
47. Kurowska-Stolarska M, Stolarski B, Kewin P, Murphy G, Corrigan CJ, Ying S, Pitman N, Mirchandani A, Rana B, van Rooijen N, Shepherd M, McSharry C, McInnes IB, Xu D, Liew FY: IL-33 amplifies the polarization of alternatively activated macrophages that contribute to airway inflammation. J Immunol 2009, 183:6469–6477
48. Fridlender ZG, Sun J, Kim S, Kapoor V, Cheng G, Ling L, Worthen GS, Albelda SM: Polarization of tumor-associated neutrophil phenotype by TGF-beta: "N1" versus "N2" TAN. Cancer Cell 2009, 16:183–194
49. Lisbonne M, L'Helgoualc'h A, Nauwelaers G, Turlin B, Lucas C, Herbelin A, Piquet-Pellorce C, Samson M: Invariant natural killer T-cell-deficient mice display increased CCl -induced hepatitis associated with CXCL1 over-expression and neutrophil infiltration. Eur J Immunol 2011, 41:1720–1732
50. Ahuja SK, Murphy PM: The CXC chemokines growth-regulated oncogene (GRO) alpha, GRObeta, GROgamma, neutrophil-activating peptide-2, and epithelial cell-derived neutrophil-activating peptide-78 are potent agonists for the type B, but not the type A, human interleukin-8 receptor. J Biol Chem 1996, 271:20545–20550
51. Ma C, Tarnuzzer RW, Chegini N: Expression of matrix metalloproteinases and tissue inhibitor of matrix metalloproteinases in mesothelial cells and their regulation by transforming growth factor-beta1. Wound Repair Regen 1999, 7:477–485
52. Morty RE, Königshoff M, Eickelberg O: Transforming growth factor-beta signaling across ages: from distorted lung development to chronic obstructive pulmonary disease. Proc Am Thorac Soc 2009, 6:607–613
53. Keely S, Talley NJ, Hansbro PM: Pulmonary-intestinal cross-talk in mucosal inflammatory disease. Mucosal Immunol 2012, 5:7–18
54. Adler A, Cieslewicz G, Irvin CG: Unrestrained plethysmography is an unreliable measure of airway responsiveness in BALB/c and C57BL/6 mice. J Appl Physiol 2004, 97:286–292
55. Königshoff M, Uhl F, Gosens R: From molecule to man: integrating molecular biology with whole organ physiology in studying respiratory disease. Pulm Pharmacol Ther 2011, 24:466–470
56. Lederer DJ, Arcasoy SM: Update in surgical therapy for chronic obstructive pulmonary disease. Clin Chest Med 2007, 28:639–653, vii
57. Meyers BF, Patterson GA: Chronic obstructive pulmonary disease. 10: Bullectomy, lung volume reduction surgery, and transplantation for patients with chronic obstructive pulmonary disease. Thorax 2003, 58:634–638
58. Greene CM, Hassan T, Molloy K, McElvaney NG: The role of proteases, endoplasmic reticulum stress and SERPINA1 heterozygosity in lung disease and alpha-1 anti-trypsin deficiency. Expert Rev Respir Med 2011, 5:395–411
59. Königshoff M, Kneidinger N, Eickelberg O: TGF-beta signaling in COPD: deciphering genetic and cellular susceptibilities for future therapeutic regimen. Swiss Med Wkly 2009, 139:554–563
60. Baraldo S, Bazzan E, Turato G, Calabrese F, Beghé B, Papi A, Maestrelli P, Fabbri LM, Zuin R, Saetta M: Decreased expression of TGF-beta type II receptor in bronchial glands of smokers with COPD. Thorax 2005, 60:998–1002
61. Pons AR, Sauleda J, Noguera A, Pons J, Barceló B, Fuster A, Agusti AG: Decreased macrophage release of TGF-beta and TIMP-1 in chronic obstructive pulmonary disease. Eur Respir J 2005, 26:60–66